

Sparsity-Based STAP Design Based on Alternating Direction Method with Gain/Phase Errors

Zhaocheng Yang, *Member IEEE*, Rodrigo C. de Lamare, *Senior Member IEEE*, and Weijian Liu *Member IEEE*

Abstract—We present a novel sparsity-based space-time adaptive processing (STAP) technique based on the alternating direction method to overcome the severe performance degradation caused by array gain/phase (GP) errors. The proposed algorithm reformulates the STAP problem as a joint optimization problem of the spatio-Doppler profile and GP errors in both single and multiple snapshots, and introduces a target detector using the reconstructed spatio-Doppler profiles. Simulations are conducted to illustrate the benefits of the proposed algorithm.

I. INTRODUCTION

Ground moving target detection (GMTD) in surveillance airborne radar is a crucial task for many military and civilian applications. The technique of moving target indication (MTI) exploits the differences of the Doppler frequencies between the targets and clutter for the detection of targets [1]. However, targets are often obscured by the spreading Doppler spectrum of the clutter due to the moving airborne platform, which leads to severe detection performance degradation. Unlike MTI, space-time adaptive processing (STAP) separates the target and clutter from a joint spatio-Doppler dimension, and exploits significantly more degrees of freedom (DoFs) than MTI to mitigate clutter while preserving target energy [1], [2].

Because of the large number of space-time DoFs, full rank STAP techniques have a slow convergence and requires a large number of independent and identically distributed (IID) training snapshots (e.g., twice the system DoFs according to the Reed-Mallett-Brennan rule [1], [2]), which is difficult to satisfy in real scenarios, especially in nonhomogeneous environments [1], [2]. For example, to ensure a loss less than 3dB, it requires the ground with the range of 6 kilometers to satisfy the homogeneity for a range resolution of 30 meters (corresponding to a bandwidth of 5MHz), 10 antenna elements and 10 pulses. When the observation area is the city or the sea, the above requirement is very difficult to be satisfied. Reduced-dimension and reduced-rank methods [9]–[15], [17]–[29], [29]–[36], [38]–[40], [40]–[59], including the principle-components (PC) methods [3], joint-domain localized approach [4], cross-spectral metric method [5], multistage Wiener filter [6], auxiliary-vector filtering [7], and joint interpolation, decimation and filtering algorithm

[60], have been developed to counteract the slow convergence of full rank STAP. The parametric adaptive matched filter (PAMF) based on a multichannel autoregressive model [61] and sparse space-time beamformers exploiting the sparsity of the received data and filter weights [62], [63] provide alternative solutions to reduce the number of required IID snapshots. Recently, knowledge-aided (KA) STAP techniques, which aim at exploiting environmental knowledge, have been developed to enhance the detection performance especially in the case of nonhomogeneous environments (see, e.g., [64]–[69] and the references therein). However, the exact form of prior knowledge is still problem-dependent and hard to derive. Moreover, how to effectively use the prior knowledge remains a topic for further investigation. Direct data domain least-squares (D3-LS) STAP approaches use only the received data in the cell under test (CUT) and require no training data, thereby avoiding estimation distortion caused by different statistics of the training data [70], [71]. However, this benefit comes at the cost of a reduced system DOFs resulting in degraded performance.

More recently, motivated by compressive sensing techniques, sparsity-based STAP has been applied to GMTD and its basic idea is to formulate the observing scene with the target and clutter [72]–[76], [78], [79], only the clutter [67], [79]–[87] or only the target [79], [88]–[90] estimation problem as a sparse recovery/representation (SR) problem or a low-rank matrix estimation problem [84]. Compared with conventional reduced-dimension and reduced-rank STAP algorithms, the sparsity-based STAP algorithms provide high-resolution of the scene and exhibit much better performance in a very small training support, or even in a single snapshot. However, this approach relies on the accuracy of the sparse model and suffers performance degradation due to the model mismatches caused by array errors or the intrinsic clutter motion (ICM)¹. A sparsity-based D3 STAP algorithm with the covariance matrix taper (CMT) has been proposed to overcome the model mismatches caused by the ICM [78]. A sparsity-based STAP with array gain/phase (GP) error self-calibration has been developed in [87], which iteratively solves an SR problem and an LS calibration problem. Since it requires to repeatedly recover the scene in every iteration, the computational complexity is high.

¹One point worth mentioning is that standard STAP is relative robust because these errors are captured in the adaptively estimated space-time covariance matrix if assuming that they are constant over the coherent processing interval and things are suitably narrowband. The only impact to detection is a potential loss of the output signal-to-interference-plus-noise ratio (SINR) from steering vector mismatch.

Z. Yang is with College of Information Engineering, Shenzhen University, Shenzhen, Guangdong, 518060, China. Email: yangzhaocheng@szu.edu.cn. R. C. de Lamare is with Department of Electronics, University of York, YO10 5DD, York, UK. Email: delamare@cetuc.puc-rio.br. W. Liu is with Wuhan Radar Academy, Wuhan 430019, China. Email: liuvjian@163.com

This work was supported in part by National Natural Science Foundation of China under Grant 61401478, the Science & Technology Innovation Project of Shenzhen under Grant JCYJ20160307112710376 and the Natural Science Foundation of SZU under Grant 2016056.

In this paper, we focus on the GMTD using the sparsity-based STAP in the presence of array GP errors. We first build the sparse measurement model by taking array GP errors into account. Under the framework of the alternating direction method (ADM) [91], [92], we add a constraint to the array GP errors, and transform the conventional sparsity-based STAP problem into a joint optimization problem of the spatio-Doppler profile and the array GP errors. Different from the conventional sparsity-based STAP, the proposed algorithm simultaneously estimates the spatio-Doppler profile and array GP errors resulting in adaptation to practical situations. Unlike the approach in [87], the proposed algorithm only requires the recovery procedure once, leading to a reduced computational complexity. Furthermore, we propose iterative approaches to solve the above problem with both single snapshot and multiple snapshots. A median constant false alarm (CFAR) detector based on the reconstructed spatio-Doppler profiles is developed for target detection. Finally, simulations are carried out to illustrate the performance and computational complexity of the proposed algorithm.

The work is organized as follows. Section II introduces the STAP signal model in the presence of array GP errors for airborne radar systems. Section III builds the sparse signal model, and details the sparsity-based STAP using the ADM framework. Simulated airborne radar data are used to evaluate the performance of the proposed algorithm in Section IV. Section V provides the summary and conclusions.

Notation: scalar quantities are denoted with italic typeface. Lowercase boldface quantities denote vectors and uppercase boldface quantities denote matrices. The operations of transposition, complex conjugation, and conjugate transposition are denoted by superscripts T , $*$, and H , respectively. The symbols \otimes , \odot , $|\cdot|$, $\Re[\cdot]$, and $\|\cdot\|_p$ represent the Kronecker product, Hadamard product, absolute value, real part of the argument, and l_p -norm operation, respectively.

II. SIGNAL MODEL

The airborne radar system under consideration employs a uniform linear array (ULA) consisting of M antenna elements with half wavelength inner spacing $d_a = \lambda_c/2$ (where λ_c is the carrier wavelength), as shown in Fig.1. Each element receives N pulses in a coherent processing interval (CPI) with the pulse repetition interval (PRI) of T_r . At the receiver, each antenna element has its own low-noise amplifier (LNA), mixer and AD converter (ADC). After these, all samples (NM) from the same CPI are combined for sequential processing. In general, the target detection problem for airborne radar can be stated in the context of binary hypothesis testing as given by

$$\begin{aligned} H_0 : \mathbf{x} &= \mathbf{x}_u \\ H_1 : \mathbf{x} &= \mathbf{x}_t + \mathbf{x}_u, \end{aligned} \quad (1)$$

where \mathbf{x}_t is the target component, \mathbf{x}_u is the disturbance component, H_0 and H_1 denote target-absence and target-presence, respectively. In reality, as the external environment changes, such as temperature and humidity, the consistency of the amplifiers of the array multi-channel receivers is hard to keep. This inconsistency of the amplifiers is usually modeled

as the array GP errors [2]. Hence, for a point target, \mathbf{x}_t can be written as

$$\mathbf{x}_t = \alpha_t \mathbf{v}_d(f_d^t) \otimes (\mathbf{c} \odot \mathbf{v}_s(f_s^t)) = \alpha_t \mathbf{C} \mathbf{v}(f_d^t, f_s^t) \quad (2)$$

where $\mathbf{c} = [c_1, \dots, c_M]^T$ is the $M \times 1$ array GP error vector, $\mathbf{C} = \mathbf{I}_N \otimes \text{diag}(\mathbf{c})$, \mathbf{I}_N is an identity matrix of size N , $\mathbf{v}_d(f_d^t)$ denotes the $N \times 1$ temporal steering vector at the target Doppler frequency f_d^t , $\mathbf{v}_s(f_s^t)$ denotes the spatial steering vector in the direction provided by the target spatial frequency f_s^t , and $\mathbf{v}(f_d^t, f_s^t) = \mathbf{v}_d(f_d^t) \otimes \mathbf{v}_s(f_s^t)$ is the space-time steering vector without array GP error. For the ULA, the steering vectors $\mathbf{v}_s(f_s^t)$ and $\mathbf{v}_d(f_d^t)$ are given by

$$\mathbf{v}_s(f_s^t) = [1, \exp(j2\pi f_s^t), \dots, \exp(j2(M-1)\pi f_s^t)]^T, \quad (3)$$

$$\mathbf{v}_d(f_d^t) = [1, \exp(j2\pi f_d^t), \dots, \exp(j2(N-1)\pi f_d^t)]^T. \quad (4)$$

The disturbance vector \mathbf{x}_u is composed of the clutter component \mathbf{x}_c and the thermal noise component \mathbf{n} , i.e., $\mathbf{x}_u = \mathbf{x}_c + \mathbf{n}$. It is usually assumed that the clutter can be adequately approximated by a summation of individual clutter patches over the iso-range of interest, given by

$$\begin{aligned} \mathbf{x}_c &= \sum_{k=1}^{N_c} \alpha_{c,k} \mathbf{v}_d(f_{d,k}^c) \otimes (\mathbf{c} \odot \mathbf{v}_s(f_{s,k}^c)) \\ &= \mathbf{C} \sum_{k=1}^{N_c} \alpha_{c,k} \mathbf{v}(f_{d,k}^c, f_{s,k}^c), \end{aligned} \quad (5)$$

where N_c denotes the number of independent clutter patches, $\alpha_{c,k}$ is the random complex amplitude of the k th clutter patch, and $f_{s,k}^c$ and $f_{d,k}^c$ are the spatial and Doppler frequencies, respectively, of the k th clutter patch. Moreover, it is assumed that the clutter amplitudes $\alpha_{c,k}$, $k = 1, 2, \dots, N_c$, are IID mean-zero complex Gaussian random variables with variance $\sigma_{c,k}^2$. Hence, the corresponding clutter covariance matrix can be represented by

$$\mathbf{R}_c = \mathbf{C} \sum_{k=1}^{N_c} \sigma_{c,k}^2 \mathbf{v}(f_{d,k}^c, f_{s,k}^c) \mathbf{v}^H(f_{d,k}^c, f_{s,k}^c) \mathbf{C}^H. \quad (6)$$

Additionally, we assume that the clutter spectral characteristics follow the local homogeneity. In the following, we will use this local homogeneity to estimate the clutter-plus-noise power level for target detection. Since the thermal noise comes from the receiver electronics and is added to the return after it passes through the antenna array, it is not affected by the array errors. Here, we assume the thermal noise \mathbf{n} is independent from element to element and from pulse to pulse and follows the zero-mean Gaussian distribution with covariance matrix $\mathbf{R}_n = \sigma_n^2 \mathbf{I}_{NM}$.

III. PROPOSED SPARSITY-BASED STAP IN THE PRESENCE OF ARRAY GP ERRORS

In this section, we first introduce the sparse signal model in the presence of array GP errors, and then detail the sparsity-based STAP algorithm under the framework of ADM.

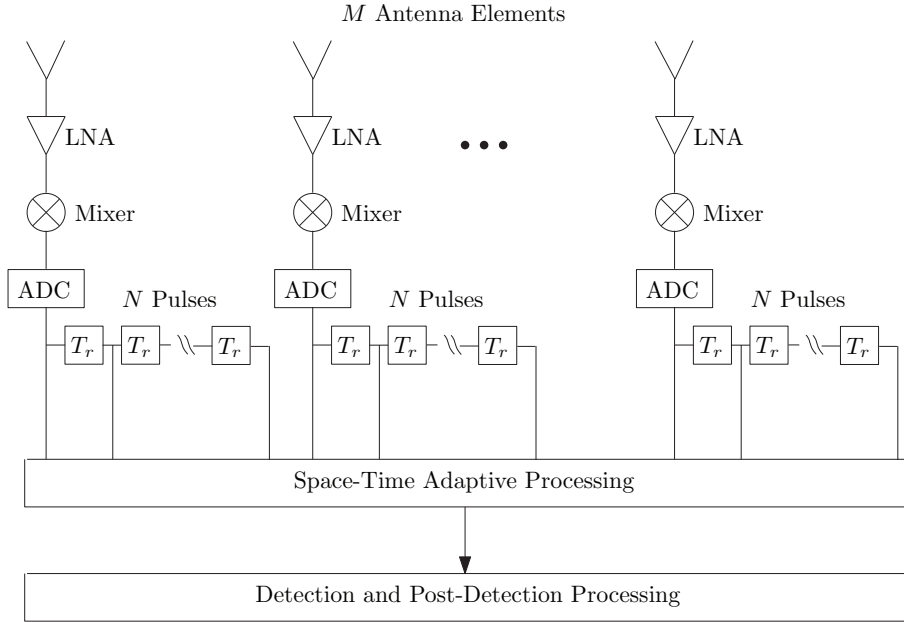


Fig. 1. A general block diagram for a space-time processor.

A. Sparse Signal Model

One notes that the clutter return in (5) is a function of the Doppler frequency and spatial frequency. Let us discretize the whole spatio-Doppler plane into a large number of grid points (where $N_s = \rho_s M$, $N_d = \rho_d N$, $\rho_s, \rho_d > 1$, N_s and N_d are the discretized number of grid points along the spatial and Doppler frequencies, respectively) [72]. A nonzero element from any such grid point would suggest the presence of a scatterer at that particular spatial and Doppler frequencies. We denote the discretized spatial and Doppler frequencies of all grid points as $\Psi = \{(f_{d,1}, f_{s,1}), (f_{d,1}, f_{s,2}), \dots, (f_{d,N_d}, f_{s,N_s})\}$. Therefore, the spatial and Doppler frequencies of the N_c clutter patches can be seen as a subset of Ψ , termed as Ψ_c . Hence, similar to (5), the clutter return can be expressed by

$$\mathbf{x}_c = \mathbf{C}\Phi\alpha_c, \quad (7)$$

where $\alpha_c = [\alpha_{1,1}, \alpha_{1,2}, \dots, \alpha_{N_d, N_s}]^T$ denotes the $N_d N_s \times 1$ spatio-Doppler profile with nonzero elements representing the clutter, and the $NM \times N_d N_s$ matrix Φ is the over-complete space-time steering dictionary, as given by

$$\Phi = [\mathbf{v}(f_{d,1}, f_{s,1}), \mathbf{v}(f_{d,1}, f_{s,2}), \dots, \mathbf{v}(f_{d,N_d}, f_{s,N_s})], \quad (8)$$

The clutter sparsity can be understood from the following two points: (a) it is well known that, the relationship between the Doppler frequency and the spatial frequency is a one-to-one mapping. For example, the shapes of the clutter ridge are straight lines for the side-looking ULA. Compared with the whole discretized place (corresponding to the size of the set Ψ), the number of the nonzero elements in the spatio-Doppler profile occupied by the clutter (corresponding to the size of the subset Ψ_c) is quite small. (b) It is proved that for the case of side-looking radar with a ULA, constant PRF, constant platform velocity and no crab angle, there is a group of space-time steering vectors (whose number is

equivalent to the clutter rank) that can approximately represent the clutter subspace [81]. That is to say the clutter sparsity is much lower than the system DoFs and far lower than $N_d N_s$ (since the clutter rank is much lower than NM and $NM \gg N_d N_s$). Similar conclusions are also obtained by L. Bai [77]. Moreover, according to [8], the clutter rank can be estimated by counting the number of resolution grids that are occupied by the significant clutter spectrum components. Therefore, there is a high degree of sparsity of the clutter in the spatio-Doppler profile.

When a target is present in the CUT, corresponding to H_1 hypothesis, the target's return is just like the response of a nonzero element in the spatio-Doppler profile. If we assume the target's spatial and Doppler frequencies are from the grid points Ψ , then, the target return can be written as

$$\mathbf{x}_t = \mathbf{C}\Phi\alpha_t, \quad (9)$$

where α_t denotes the target amplitude. Thus, the total return in the presence of target can be represented by

$$\mathbf{x} = \mathbf{x}_t + \mathbf{x}_c + \mathbf{n} = \mathbf{C}\Phi\alpha + \mathbf{n}, \quad (10)$$

where $\alpha = \alpha_t + \alpha_c$ represent the amplitudes from both the clutter and the target. Because of the limitation of the number of targets, it results in sparsity of the spatio-Doppler profile.

B. Problem Formulation via the Framework of ADM

For simplicity and convenience, we rewrite the expression of (10) as

$$\mathbf{T}\mathbf{x} = \Phi\alpha + \mathbf{n}'. \quad (11)$$

where $\mathbf{T} = \mathbf{I}_N \otimes \text{diag}(\mathbf{t})$, $\mathbf{t} = [t_1, \dots, t_M]^T$, $t_m = c_m^{-1}$, $1 \leq m \leq M$, and $\mathbf{n}' = \mathbf{T}\mathbf{n}$. Here, we assume that the unknown array GP errors are nonzeros. Exploiting the sparsity of α , the spatio-Doppler profile can be approximately estimated by

solving the so-called basis pursuit denoising (BPDN) problem, described by

$$\min_{\alpha} \|\alpha\|_1 + \frac{1}{2\rho} \|\mathbf{T}\mathbf{x} - \Phi\alpha\|_2^2, \quad (12)$$

where $\rho > 0$ is the positive regularization parameter that provides a trade-off between the sparsity and total squared error. With an auxiliary variable $\mathbf{r} = \mathbf{T}\mathbf{x} - \Phi\alpha$, the above BPDN problem can be reformulated as

$$\begin{aligned} \min_{\alpha, \mathbf{r}} \|\alpha\|_1 + \frac{1}{2\rho} \|\mathbf{r}\|_2^2 \\ \text{s.t. } \Phi\alpha + \mathbf{r} = \mathbf{T}\mathbf{x} \end{aligned} \quad (13)$$

Then, the augmented Lagrangian function of this problem is given by [91], [92]

$$\begin{aligned} \min_{\alpha, \mathbf{r}, \lambda, \mathbf{t}} \mathcal{L}'(\alpha, \mathbf{r}, \lambda, \mathbf{t}) = \min_{\alpha, \mathbf{r}, \lambda, \mathbf{t}} \|\alpha\|_1 + \frac{1}{2\rho} \|\mathbf{r}\|_2^2 \\ - \Re \left\{ \lambda^H (\Phi\alpha + \mathbf{r} - \mathbf{T}\mathbf{x}) \right\} + \frac{\beta}{2} \|\Phi\alpha + \mathbf{r} - \mathbf{T}\mathbf{x}\|_2^2 \end{aligned} \quad (14)$$

where $\lambda \in \mathbb{C}^{NM}$ is a Lagrange multiplier and $\beta > 0$ is a penalty parameter. Note that the matrix \mathbf{T} of (14) depends on the array GP error vector $\mathbf{c}(\mathbf{t})$, which is unknown and should be estimated from the data. Given the snapshot \mathbf{x} and the over-complete space-time steering dictionary Φ , we can obtain the spatio-Doppler profile α , the auxiliary variable \mathbf{r} and the array GP error vector \mathbf{c} by applying alternating minimization to solve (14).

With the above formulation, we observe that the problem (14) is an unconstrained convex optimization problem. However, it is trivially satisfied for zeros of vectors \mathbf{t} and α . To avoid this trivial solution, we introduce a convex normalization constraint $\sum_{m=1}^M t_m = \varsigma$, where $\varsigma \in \mathbb{C}$ is an arbitrary constant scale. Therefore, the cost function $\mathcal{L}'(\alpha, \mathbf{r}, \lambda, \mathbf{t})$ in problem (14) can be rewritten as

$$\begin{aligned} \mathcal{L}(\alpha, \mathbf{r}, \lambda, \mathbf{t}) = \|\alpha\|_1 + \frac{1}{2\rho} \|\mathbf{r}\|_2^2 - \Re \left\{ \gamma^* \left(\sum_{m=1}^M t_m - \varsigma \right) \right\} \\ - \Re \left\{ \lambda^H (\Phi\alpha + \mathbf{r} - \mathbf{T}\mathbf{x}) \right\} + \frac{\beta}{2} \|\Phi\alpha + \mathbf{r} - \mathbf{T}\mathbf{x}\|_2^2 \end{aligned} \quad (15)$$

where γ is a Lagrange multiplier. The actual array GP error vector is recovered after the optimization using $c_m = 1/t_m$, $m = 1, \dots, M$. One should also note that the estimated array GP error vector scales to the true one because of the constant scale ς in the constraint.

C. Jointly Iterative Estimation of the Spatio-Doppler Profile and Array GP Error

In this subsection, we estimate the spatio-Doppler profile and array GP error vector iteratively. For $\alpha = \alpha^p$, $\lambda = \lambda^p$, and $\mathbf{t} = \mathbf{t}^p$ fixed ($()^p$ denotes the p th iteration), the minimizer of (15) with respect to \mathbf{r}^* is given by

$$\mathbf{r}^{p+1} = \frac{\rho\beta}{1 + \rho\beta} \left(\frac{\lambda^p}{\beta} - \Phi\alpha^p + \mathbf{T}^p\mathbf{x} \right). \quad (16)$$

Similarly, for $\mathbf{r} = \mathbf{r}^{p+1}$, $\lambda = \lambda^p$, and $\mathbf{t} = \mathbf{t}^p$ fixed, the minimization of (15) with respect to α^* is equivalent to

$$\min_{\alpha} \|\alpha\|_1 + \frac{\beta}{2} \left\| \Phi\alpha + \mathbf{r}^{p+1} - \mathbf{T}^p\mathbf{x} - \frac{\lambda^p}{\beta} \right\|_2^2. \quad (17)$$

Then, the solution of the problem (17) can be approximately given by [91], [92]

$$\begin{aligned} \alpha^{p+1} &= \text{soft} \left(\alpha^p - \tau \mathbf{g}^p, \frac{\tau}{\beta} \right) \\ &= \max \left\{ |\alpha^p - \tau \mathbf{g}^p| - \frac{\tau}{\beta}, 0 \right\} \frac{\alpha^p - \tau \mathbf{g}^p}{|\alpha^p - \tau \mathbf{g}^p|}, \end{aligned} \quad (18)$$

where all the operations in (18) are performed component-wise (usually known as shrinkage), $\frac{0}{0} = 0$, $\tau > 0$ is a proximal parameter and

$$\mathbf{g}^p = \Phi^H \left(\Phi\alpha^p + \mathbf{r}^{p+1} - \mathbf{T}^p\mathbf{x} - \frac{\lambda^p}{\beta} \right). \quad (19)$$

Given $\mathbf{r} = \mathbf{r}^{p+1}$, $\lambda = \lambda^p$ and $\alpha = \alpha^{p+1}$, the minimization of (15) with respect to \mathbf{t}^* can be simplified as

$$\begin{aligned} \min_{\mathbf{t}} \frac{\beta}{2} \left\| \Phi\alpha^{p+1} + \mathbf{r}^{p+1} - \mathbf{T}\mathbf{x} - \frac{\lambda^p}{\beta} \right\|_2^2 \\ - \Re \left\{ \gamma^* \left(\sum_{m=1}^M t_m - \varsigma \right) \right\} \end{aligned} \quad (20)$$

For simplicity, we denote $\mathbf{z}^p = \Phi\alpha^{p+1} + \mathbf{r}^{p+1} - \frac{\lambda^p}{\beta}$, $\mathbf{T}\mathbf{x} = \mathbf{Q}\mathbf{t}$ and $\mathbf{Q} = \text{diag}(\mathbf{x})(\mathbf{1}_N \otimes \mathbf{I}_M)$. Then, (20) can be rewritten with the form of

$$\min_{\mathbf{t}} \frac{\beta}{2} \|\mathbf{z}^p - \mathbf{Q}\mathbf{t}\|_2^2 - \Re \left\{ \gamma^* \left(\sum_{m=1}^M t_m - \varsigma \right) \right\}. \quad (21)$$

By taking the gradient of the cost function in problem (21) with respect to \mathbf{t}^* and γ^* , equating the terms to zero, and solving for \mathbf{t} , we obtain (the detailed derivations are given in Appendix A)

$$\mathbf{t}^{p+1} = \left[\frac{b_1 + \gamma}{a_1}, \frac{b_2 + \gamma}{a_2}, \dots, \frac{b_M + \gamma}{a_M} \right]^T, \quad (22)$$

where b_m , a_m and γ , ($m = 1, 2, \dots, M$) are defined by (41), (42) and (43) in Appendix A.

Finally, minimizing (15) with respect to λ^* , we obtain the update of the multiplier λ as

$$\lambda^{p+1} = \lambda^p - \beta (\Phi\alpha^{p+1} + \mathbf{r}^{p+1} - \mathbf{T}^{p+1}\mathbf{x}). \quad (23)$$

In short, the proposed approach iteratively updates (16), (18), (22) and (23) to obtain estimates of the spatio-Doppler profile and array GP error vector.

D. Application to Multiple Snapshots

It is reasonable to suppose that the array GP errors are identical for different snapshots from adjacent range bins in the same CPI. By using multiple snapshots, we can expect to improve the accuracy of the estimated array GP errors and spatio-Doppler profiles. In the following, we apply the proposed ADM algorithm to the multiple snapshots case. For

L snapshots, \mathbf{x}_l , $l = 1, 2, \dots, L$, the problem of (15) can be reformulated as

$$\begin{aligned} \min_{\alpha_l, \mathbf{r}_l, \mathbf{t}_l} & \sum_{l=1}^L \|\alpha_l\|_1 + \frac{1}{2\rho} \sum_{l=1}^L \|\mathbf{r}_l\|_2^2 \\ & - \Re \left\{ \sum_{l=1}^L \lambda_l^H (\Phi \alpha_l + \mathbf{r}_l - \mathbf{T} \mathbf{x}_l) \right\} \\ & + \frac{\beta}{2} \sum_{l=1}^L \|\Phi \alpha_l + \mathbf{r}_l - \mathbf{T} \mathbf{x}_l\|_2^2 - \Re \left\{ \gamma^* \left(\sum_{m=1}^M t_m - \varsigma \right) \right\}, \end{aligned} \quad (24)$$

where α_l , \mathbf{r}_l and λ_l denote the corresponding variables of the l th snapshot.

Let us define $\Upsilon = [\alpha_1, \alpha_2, \dots, \alpha_L]$, $\Gamma = [\mathbf{r}_1, \mathbf{r}_2, \dots, \mathbf{r}_L]$, $\Lambda = [\lambda_1, \lambda_2, \dots, \lambda_L]$, and $\mathbf{X} = [\mathbf{x}_1, \mathbf{x}_2, \dots, \mathbf{x}_L]$. Similar to the derivations in the previous subsection, we can subsequently obtain the updates of Υ , Γ and Λ as

$$\Gamma^{p+1} = \frac{\rho\beta}{1+\rho\beta} \left(\frac{\Lambda^p}{\beta} - \Phi \Upsilon^p + \mathbf{T}^p \mathbf{X} \right), \quad (25)$$

$$\Upsilon^{p+1} = \text{soft} \left(\Upsilon^p - \tau \mathbf{G}^p, \frac{\tau}{\beta} \right), \quad (26)$$

and

$$\Lambda^{p+1} = \Lambda^p - \beta (\Phi \Upsilon^{p+1} + \Gamma^{p+1} - \mathbf{T}^{p+1} \mathbf{X}), \quad (27)$$

where

$$\mathbf{G}^p = \Phi^H \left(\Phi \Upsilon^p + \Gamma^{p+1} - \mathbf{T}^p \mathbf{X} - \frac{\Upsilon^p}{\beta} \right). \quad (28)$$

The update of the vector \mathbf{t} with multiple snapshots case can be represented by

$$\mathbf{t}^{p+1} = \left[\frac{\sum_{l=1}^L b_{l,1} + \tilde{\gamma}}{\sum_{l=1}^L a_{l,1}}, \dots, \frac{\sum_{l=1}^L b_{l,M} + \tilde{\gamma}}{\sum_{l=1}^L a_{l,M}} \right]^T, \quad (29)$$

where

$$b_{l,m} = \sum_{n=1}^L \sum_{n=1}^N x_{l,(n-1)M+m}^* z_{l,(n-1)M+m}^p, \quad (30)$$

$$a_{l,m} = \sum_{n=1}^L \sum_{n=1}^N |x_{l,(n-1)M+1}|^2, \quad (31)$$

$$\tilde{\gamma} = \frac{\varsigma - \sum_{m=1}^M \frac{\sum_{l=1}^L b_{l,m}}{\sum_{l=1}^L a_{l,m}}}{\sum_{m=1}^M \frac{1}{\sum_{l=1}^L a_{l,m}}}, \quad (32)$$

and

$$\mathbf{Z}^p = [\mathbf{z}_1^p, \mathbf{z}_2^p, \dots, \mathbf{z}_L^p] = \Phi \Upsilon^{p+1} + \Gamma^{p+1} - \frac{\Lambda^p}{\beta}. \quad (33)$$

Moreover, we detail the proposed ADM algorithm for jointly iterative estimation of the spatio-Doppler profile and the array GP error vector (shortened as JIE-ADM) in Table I.

TABLE I
THE PROPOSED JIE-ADM ALGORITHM

Initialization:	
$\alpha_l^0 = \mathbf{0}_{N_d N_s}$, $\lambda_l^0 = \mathbf{0}_{NM}$, $l = 1, \dots, L$,	
$\mathbf{t}^0 = \mathbf{1}_M$, $\mathbf{T}^0 = \mathbf{I}_N \otimes \text{diag}(\mathbf{t}^0)$, $p = 0$	
Repeat	
1	$\Gamma^{p+1} = \frac{\rho\beta}{1+\rho\beta} \left(\frac{\Lambda^p}{\beta} - \Phi \Upsilon^p + \mathbf{T}^p \mathbf{X} \right)$,
2	$\mathbf{G}^p = \Phi^H \left(\Phi \Upsilon^p + \Gamma^{p+1} - \mathbf{T}^p \mathbf{X} - \frac{\Upsilon^p}{\beta} \right)$,
3	$\Upsilon^{p+1} = \text{soft} \left(\Upsilon^p - \tau \mathbf{G}^p, \frac{\tau}{\beta} \right)$,
4	Update \mathbf{Z}^p , $b_{l,m}$, $a_{l,m}$ and $\tilde{\gamma}$ by (33), (30) (31), and (32),
5	$\mathbf{t}^{p+1} = \left[\frac{\sum_{l=1}^L b_{l,1} + \tilde{\gamma}}{\sum_{l=1}^L a_{l,1}}, \dots, \frac{\sum_{l=1}^L b_{l,M} + \tilde{\gamma}}{\sum_{l=1}^L a_{l,M}} \right]^T$
6	$\Lambda^{p+1} = \Lambda^p - \beta (\Phi \Upsilon^{p+1} + \Gamma^{p+1} - \mathbf{T}^{p+1} \mathbf{X})$,
Until	$\frac{\sum_{l=1}^L \ \alpha_l^p - \alpha_l^{p+1}\ _2}{\sum_{l=1}^L \ \alpha_l^{p+1}\ _2} \leq \varsigma$

E. Target Detection

Since the main purpose of this paper is to improve the spatio-Doppler profiles' estimation by using the joint estimation approach, in this subsection, we only consider using a simple detector for illustration purposes. Furthermore, following the ideas in [74], we focus on target detection based on the estimated spatio-Doppler profiles. It is reasonable to assume that the reconstructed clutter peaks at a few (say, 10) adjacent range bins are nearly the same, and the target peaks are not so "dense" in range [74]. Therefore, as shown in Fig.2, we first exclude some snapshots around the CUT (namely the guard cells) for avoiding target canceling, and then perform a moving test window to the estimated spatio-Doppler profile $\hat{\alpha}_{\text{CUT}}$ at the CUT with the size of a spatio-Doppler resolution cell (i.e., $1/N$ and $1/M$ for the Doppler and spatial frequencies, respectively). When we conduct the detection procedure, we should determine the presence/absence of the target for every single angle and every single Doppler frequency. Since the airborne radar transmitter usually keeps a high gain in the observing angle for a CPI, we only require to conduct the detection procedure by fixing the spatial frequency of detection to the main-lobe $f_s^{t_0}$ and varying the Doppler frequency within a set of possible values. Specifically, for a possible target Doppler frequency f_d^t , the range of the moving test window is $(f_d^t - 1/2N, f_d^t + 1/2N)$ and $(f_s^{t_0} - 1/2M, f_s^{t_0} + 1/2M)$. Then, we pick out the elements that belong to the moving test window from $\hat{\alpha}_{\text{CUT}}$, and arrange them into a new vector $\tilde{\alpha}_{\text{CUT}}$, as given by

$$\tilde{\alpha}_{\text{CUT}} = \left\{ \hat{\alpha}_{\text{CUT},k,i} \left| f_{d,k} \in \left(f_d^t - \frac{1}{2N}, f_d^t + \frac{1}{2N} \right), \right. \right. \\ \left. \left. f_{s,i} \in \left(f_s^{t_0} - \frac{1}{2M}, f_s^{t_0} + \frac{1}{2M} \right) \right\}, \quad (34)$$

Similarly, for the same moving test window, we form L secondary samples $\tilde{\alpha}_l$, $l = 1, 2, \dots, L$, by

$$\tilde{\alpha}_l = \left\{ \hat{\alpha}_{l,k,i} \left| f_{d,k} \in \left(f_d^t - \frac{1}{2N}, f_d^t + \frac{1}{2N} \right), \right. \right. \\ \left. \left. f_{s,i} \in \left(f_s^{t_0} - \frac{1}{2M}, f_s^{t_0} + \frac{1}{2M} \right) \right\}, \quad (35)$$

Due to the estimation errors or the discretized errors, the target energy might be not just concentrated at a single

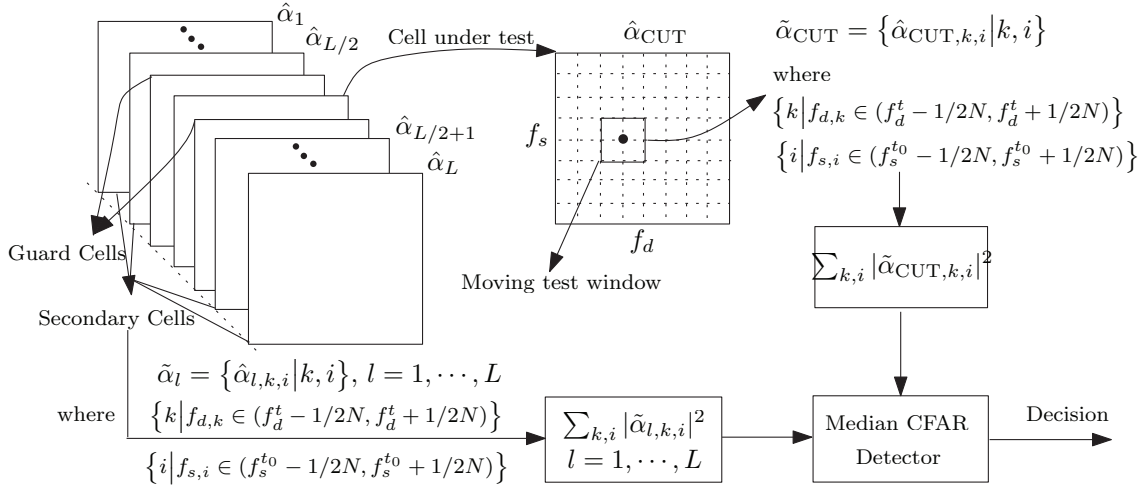


Fig. 2. The procedure of the median CFAR detector.

discretized spatio-Doppler grid point. Therefore, we select the sum value of absolute elements in $\tilde{\alpha}_{\text{CUT}}$ as the test statistic for each spatio-Doppler resolution cell. Similar operations are carried out for the secondary samples $\tilde{\alpha}_l$, $l = 1, \dots, L$, which are used to generate the background clutter-plus-noise level. Finally, we use a median CFAR detector with the form of [93]

$$20 \log \vartheta_{\text{CUT}} - 20 \log \text{median}(\vartheta_l) \underset{H_0}{\overset{H_1}{>}} \xi, \quad (36)$$

where $l = 1, 2, \dots, L$, ξ is the threshold scalar, $\text{median}(\cdot)$ yields the median value of samples in the parentheses, \log represents the logarithm taking 10 as the base, and ϑ_{CUT} and ϑ_l are given by

$$\begin{aligned} \vartheta_{\text{CUT}} &= \sum_{k,i} |\tilde{\alpha}_{\text{CUT},k,i}|, \\ \vartheta_l &= \sum_{k,i} |\tilde{\alpha}_{l,k,i}|. \end{aligned} \quad (37)$$

IV. PERFORMANCE ASSESSMENT

In this section, we evaluate the performance of the proposed JIE-ADM algorithm in terms of qualities of the reconstructed spatio-Doppler profiles and the probability of detection (PD) using simulated data. For comparison purposes, we also show the performance of the proposed JIE-ADM algorithm, conventional D3-LS STAP [70], ADM [91], basis pursuit using interior-point method (BP-IPM) [94], and IAA [74] and ADMT (using the ADM reconstructs the spatio-Doppler profile with the known array GP errors).

The parameters of the simulated radar platform are shown in Table II. In addition, for each range bin, the $[-\pi/2, \pi/2]$ AOA interval was divided into 361 clutter patches, whose single channel, single pulse clutter-to-noise ratio (CNR) is 30dB. The thermal noise power for each channel and each pulse is set to unit. The gain error and phase error are both assumed to follow a uniform distribution [68], [87]. Specifically, we can denote the m th entry of the array GP error vector as $c_m = (1 + \epsilon_m)e^{j\phi_m}$, $m = 1, 2, \dots, M$, where ϵ_m and ϕ_m follow a

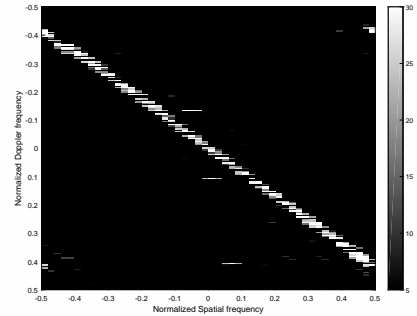


Fig. 3. The reconstructed spatio-Doppler profiles with array GP errors $\epsilon_{\text{max}} = 0.1$ and $\phi_{\text{max}} = 0.1\pi$ when the number of transmitted pulses is 100.

uniform distribution within $[-\epsilon_{\text{max}}, \epsilon_{\text{max}}]$ and $[-\phi_{\text{max}}, \phi_{\text{max}}]$, respectively.

Additionally, in the following simulations, for the JIE-ADM and ADM algorithms, $\beta = 0.1$, $\rho = 0.01$, $\zeta = 10^{-4}$ and the maximum iteration number 500. For the BP-IPM, the noise allowance parameter is set to 10^{-3} and the maximum iteration number 500. For the IAA, the stopping criterion is decided by both the preset limit relative change of the solutions between two adjacent iterations 10^{-4} and the maximum iteration number 20. Moreover, the whole spatio-Doppler plane is discretized into $N_d \times N_s = 5N \times 5M$ grid points for all algorithms.

TABLE II
PARAMETERS OF AIRBORNE RADAR SYSTEM

Parameter	Value
Antenna array	Side-looking ULA
Antenna array spacing	$\lambda_c/2$
Carrier frequency	1.24GHz
Transmit taper	Uniform
PRF	1984Hz
Platform velocity	100m/s
Platform height	3000 m
Antenna elements number	10
Pulse number in one CPI	10

In the first example, we focus on the spatio-Doppler profile reconstructions considering different cases of array GP errors: case 1, no array GP error, i.e., $\epsilon_{\max} = 0$ and $\phi_{\max} = 0$; case 2, $\epsilon_{\max} = 0.05$ and $\phi_{\max} = 0.05\pi$; case 3, $\epsilon_{\max} = 0.1$ and $\phi_{\max} = 0.1\pi$. In addition, we assume that there are three targets in the boresight at the range bin of interest: target 1 with the normalized Doppler frequency equal to -0.13 and the input signal-to-noise ratio (SNR) set to 0.2dB ; target 2 with the normalized Doppler frequency equal to 0.11 and the target's input SNR set to -3.8dB ; and target 3 with the normalized Doppler frequency equal to 0.41 and the target's input SNR set to -3.8dB . Here, we set a larger target's input SNR for target 1 because it stands for a slow target and is not well recovered when in small input SNR. As shown in Fig.??, we see that the spatio-Doppler profiles can be well reconstructed for the ADMT when the array GP errors are known. It is also observed that more and more pseudo peaks are present in the spatio-Doppler profiles using the ADM, BP-IPM and IAA algorithms, as the increase of the array GP errors. On the contrary, the spatio-Doppler profiles using the proposed JIE-ADM algorithm keep nearly the same qualities as those using the ADMT.

To better illustrate the performance of the proposed algorithm, we conduct simulations with a large number of pulses (i.e., 100). The reconstructed spatio-Doppler profiles with array GP errors $\epsilon_{\max} = 0.1$ and $\phi_{\max} = 0.1\pi$ are shown in Fig.3. The whole spatio-Doppler plane is discretized into $N_d \times N_s = 2N \times 5M$ grid points. Other parameters are same as those of the first example. From the images, we note that the reconstructed spatio-Doppler profiles of all considered algorithms show better performance than those when transmitting a small number of pulses (i.e., 10) in Fig.?.?. Again, we still note that the proposed algorithm exhibits similar performance with the ADMT, and much better quality than the ADM, BP-IPM and IAA algorithms. This illustrates that the proposed algorithm outperforms other algorithms, which are without array GP errors estimation, when the target is at a low speed. Additionally, one should note that the fine characteristics of clutter spectrum are important for the sparsity-based STAP algorithms. Specifically, it might have different influences on different algorithms.

In the second example, we assess the detection performance of the proposed algorithm. The false alarm rate P_{fa} is set to 10^{-3} , and the target is in the boresight with the normalized Doppler frequency 0.36 . First, in Fig.4, we show the impacts of array GP errors on the detection performance of the conventional D3-LS STAP and the existing SR algorithms, i.e., ADM, BP-IPM and IAA. In the figure, AMF-Optimum represents the detector of the adaptive matched filter (AMF) with clairvoyant knowledge of the space-time covariance matrix of the interference as well as the space-time steering vector of the target (including any "errors"). The results in Fig.4 illustrate that: (1) the detection performance of the existing SR algorithms are better than that of the conventional D3-LS STAP when there are no array GP error, which are coincident with conclusions in [76], [78]; and (2) the detection performance of the conventional D3-LS STAP and the existing SR algorithms are significantly degraded in the presence of

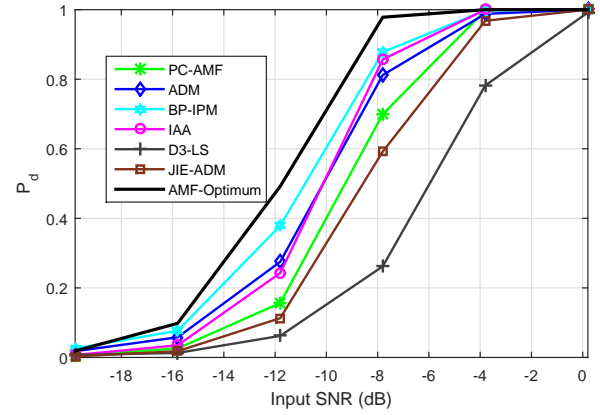


Fig. 4. Impacts of the array GP errors on the detection performance of the proposed approach and the existing ones.

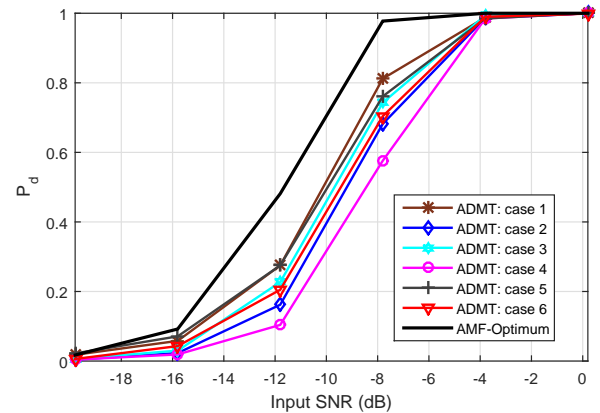


Fig. 5. The detection performance of the proposed JIE-ADM algorithm and ADMT against the target's input SNR with different cases of array GP errors: case 1, no array GP error; case 2, $\epsilon_{\max} = 0.025$ and $\phi_{\max} = 0.025\pi$; case 3, $\epsilon_{\max} = 0.05$ and $\phi_{\max} = 0.05\pi$; case 4, $\epsilon_{\max} = 0.1$ and $\phi_{\max} = 0.1\pi$; case 5, $\epsilon_{\max} = 0.15$ and $\phi_{\max} = 0.15\pi$; and case 6, $\epsilon_{\max} = 0.2$ and $\phi_{\max} = 0.2\pi$.

the array GP errors, and the proposed method achieves the best detection performance. Additionally, the performance of a typical statistical STAP method, i.e., PC, with AMF, (namely, AMF-PC) is also shown in Fig.4. The rank and the number of training snapshots used for the AMF-PC are set to 28 and 60, respectively. It illustrates that the AMF-PC is not sensitive to the array GP errors. However, statistical STAP methods require significantly more training snapshots than the sparsity-based STAP. Furthermore, in the following simulations, when the array GP errors increase, the performance of AMF-PC becomes worse than the proposed algorithm (see Fig.6).

Next, we show the detection performance of the proposed JIE-ADM algorithm and ADMT against the input SNR in Fig.5. Here, we consider six different cases of GP errors: case 1, no array GP error; case 2, $\epsilon_{\max} = 0.025$ and $\phi_{\max} = 0.025\pi$; case 3, $\epsilon_{\max} = 0.05$ and $\phi_{\max} = 0.05\pi$; case 4, $\epsilon_{\max} = 0.1$ and $\phi_{\max} = 0.1\pi$; case 5, $\epsilon_{\max} = 0.15$ and $\phi_{\max} = 0.15\pi$; and case 6, $\epsilon_{\max} = 0.2$ and $\phi_{\max} = 0.2\pi$. It is seen from Figs.4 and 5 that the proposed JIE-ADM algorithm provides slightly worse performance than the ADMT, but is more robust to the array GP errors and obtains much

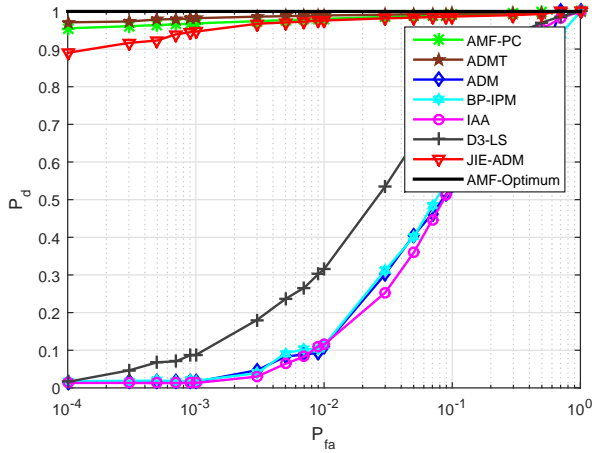


Fig. 6. The ROC curves of the proposed JIE-ADM algorithm against different Doppler frequencies at a level of array GP errors $\epsilon_{\max} = 0.1$ and $\phi_{\max} = 0.1\pi$.

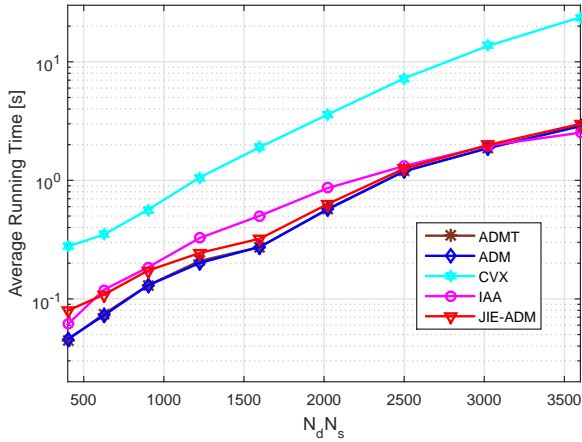


Fig. 7. The average running time of the sparsity-based STAP algorithms versus sizes of dictionary for estimating one spatio-Doppler profile.

better performance than the conventional D3-LS STAP and existing SR algorithms. This is because the proposed JIE-ADM algorithm provides more accurate estimate of the spatio-Doppler profile and is much more robust to the array GP errors.

To further investigate the performance of the proposed JIE-ADM algorithm, in Fig.6, we examine the detection performance with different Doppler frequencies at a level of array GP errors $\epsilon_{\max} = 0.1$ and $\phi_{\max} = 0.1\pi$, by showing the receiver operating characteristic (ROC) curves. Here, slow, median speed and relative fast moving targets are simulated with the normalized Doppler frequencies of 0.13, 0.23 and 0.36, respectively. The corresponding input target's SNRs are fixed to 0.2dB, -3.8 dB and -3.8 dB, respectively. The results in Fig.6 highlight that the proposed JIE-ADM algorithm considerably outperforms the conventional D3-LS STAP and existing SR algorithms in presence of array GP errors regardless of the detection of the slow, median speed or relative fast moving targets. It should be pointed out that the detection performance of the proposed algorithm degrades for the slow moving target. This can be roughly understood from Fig.?? that the difficulty to separate the target and the

clutter increases when the target is close to the clutter ridge. As the target's input SNR increases, the detection performance improves.

Fig.7 plots the average running time of the sparsity-based STAP algorithms versus sizes of dictionary for estimating one spatio-Doppler profile. Here, the simulations are operated on a standard desktop computer with a 3.6GHz CPU (dual core with Matlab's multithreading option enabled) and 4GB of memory. The size of one CPI is changed from 16 to 144, corresponding to the number of columns of the dictionary from 400 to 3600. The curves indicate that the computational complexity of the proposed JIE-ADM algorithm is close to that of the ADM and ADMT algorithms. That is to say, the added array GP errors estimation step of the proposed algorithm costs very little, which can be also concluded from the estimation equations, i.e., (40), (41), (42) and (43).

V. CONCLUSIONS

In this paper, a novel sparsity-based STAP algorithm has been presented for airborne radar. In order to avoid the performance degradation caused by array errors, the proposed algorithm reformulated the sparsity-based STAP as a joint optimization of the spatio-Doppler profile and array errors by employing the framework of ADM. By solving the above problem iteratively, we developed a median CFAR detector using the reconstructed spatio-Doppler profiles. The performance of the proposed algorithm was tested and compared with that of the conventional D3-LS STAP and other existing sparsity-based STAP algorithms. Results show that the proposed algorithm is robust to array errors and yields significant improvement in detection performance over the conventional D3-LS STAP and other existing sparsity-based STAP algorithms. Additionally, the proposed algorithm adds very little computational complexity compared with the ADM without array error estimation. In our future work, we will investigate fast sparsity-based STAP algorithms with jointly estimating the spatio-Doppler profile and array errors. Moreover, the detector design based on the spatio-Doppler profiles and its statistics will be considered and analyzed.

APPENDIX A PROOF OF (22)

Taking the gradients of the cost function in problem (21) with respect to \mathbf{t}^* and γ^* and equating them to zeros, we have

$$\mathbf{Q}^H \mathbf{Q} \mathbf{t} = \mathbf{Q}^H \mathbf{z}^p + \gamma \mathbf{1}_M, \quad (38)$$

and

$$\sum_{m=1}^M t_m = \varsigma. \quad (39)$$

Note that $\mathbf{Q}^H \mathbf{Q}$ is an $M \times M$ diagonal matrix, and its m th diagonal element is $\sum_{n=1}^N |x_{(n-1)M+m}|^2$. Thus, substituting this into (38), we obtain

$$\mathbf{t}^{p+1} = \left[\frac{b_1 + \gamma}{a_1}, \frac{b_2 + \gamma}{a_2}, \dots, \frac{b_M + \gamma}{a_M} \right]^T, \quad (40)$$

where

$$b_m = \sum_{n=1}^N x_{(n-1)M+m}^* z_{(n-1)M+m}^p, \quad (41)$$

and

$$a_m = \sum_{n=1}^N |x_{(n-1)M+1}|^2. \quad (42)$$

Substituting (40) into (39), we obtain

$$\gamma = \frac{\zeta - \sum_{m=1}^M \frac{b_m}{a_m}}{\sum_{m=1}^M \frac{1}{a_m}}, \quad (43)$$

Therefore, we have the formulation of \mathbf{t} given in (22).

REFERENCES

- [1] Ward J., Space-time adaptive processing for airborne radar, *Technical Report 1015*, MIT Lincoln laboratory, Lexington, MA, vol. Dec. 1994.
- [2] Guerci J. R., *Space-time adaptive processing for radar*. Artech House, 2003.
- [3] Haimovich A., The eigencanceler: adaptive radar by eigenanalysis methods, *IEEE Transactions on Aerospace and Electronic Systems*, vol.32, no.2, pp.532-542, Apr. 1996.
- [4] Wang H., and Cai L., On adaptive spartial-temporal processing for airborne surveillance radar systems, *IEEE Transactions on Aerospace and Electronic Systems*, vol.30, no.3, pp.660-670, 1994.
- [5] Goldstein J. S., and Reed I. S., Theory of partially adaptive radar, *IEEE Transactions on Aerospace and Electronic Systems*, vol.33, no.4, pp.1309-1325, Oct. 1997.
- [6] Goldstein J. S., Reed I. S., and Zulch P. A., Multistage Partially Adaptive STAP CFAR Detection Algorithm, *IEEE Transactions on Aerospace and Electronic Systems*, vol.35, no.2, pp.645-661, 1999.
- [7] Pados D. A., and Karystinos G. N., An iterative algorithm for the computation of the MVDR filter, *IEEE Transactions on Signal Processing*, vol.49, no.2, pp.290-300, Feb. 2001.
- [8] Wu Y., Tang J., and Peng Y., On the essence of knowledge-aided clutter covariance estimate and its convergence, *IEEE Transactions on Aerospace and Electronic Systems*, vol.47, no.1, pp.569-585, Jan. 2011.
- [9] A. M. Haimovich and Y. Bar-Ness, "An eigenanalysis interference canceler," *IEEE Trans. on Signal Processing*, vol. 39, pp. 76-84, Jan. 1991.
- [10] D. A. Pados and S. N. Batalama "Joint space-time auxiliary vector filtering for DS/CDMA systems with antenna arrays" *IEEE Transactions on Communications*, vol. 47, no. 9, pp. 1406 - 1415, 1999.
- [11] J. S. Goldstein, I. S. Reed and L. L. Scharf "A multistage representation of the Wiener filter based on orthogonal projections" *IEEE Transactions on Information Theory*, vol. 44, no. 7, 1998.
- [12] Y. Hua, M. Nikipour and P. Stoica, "Optimal reduced rank estimation and filtering," *IEEE Transactions on Signal Processing*, pp. 457-469, Vol. 49, No. 3, March 2001.
- [13] M. L. Honig and J. S. Goldstein, "Adaptive reduced-rank interference suppression based on the multistage Wiener filter," *IEEE Transactions on Communications*, vol. 50, no. 6, June 2002.
- [14] E. L. Santos and M. D. Zoltowski, "On Low Rank MVDR Beamforming using the Conjugate Gradient Algorithm", *Proc. IEEE International Conference on Acoustics, Speech and Signal Processing*, 2004.
- [15] Q. Haoli and S.N. Batalama, "Data record-based criteria for the selection of an auxiliary vector estimator of the MMSE/MVDR filter", *IEEE Transactions on Communications*, vol. 51, no. 10, Oct. 2003, pp. 1700 - 1708.
- [16] R. C. de Lamare and R. Sampaio-Neto, "Reduced-Rank Adaptive Filtering Based on Joint Iterative Optimization of Adaptive Filters", *IEEE Signal Processing Letters*, Vol. 14, no. 12, December 2007.
- [17] Z. Xu and M.K. Tsatsanis, "Blind adaptive algorithms for minimum variance CDMA receivers," *IEEE Trans. Communications*, vol. 49, No. 1, January 2001.
- [18] R. C. de Lamare and R. Sampaio-Neto, "Low-Complexity Variable Step-Size Mechanisms for Stochastic Gradient Algorithms in Minimum Variance CDMA Receivers", *IEEE Trans. Signal Processing*, vol. 54, pp. 2302 - 2317, June 2006.
- [19] C. Xu, G. Feng and K. S. Kwak, "A Modified Constrained Constant Modulus Approach to Blind Adaptive Multiuser Detection," *IEEE Trans. Communications*, vol. 49, No. 9, 2001.
- [20] Z. Xu and P. Liu, "Code-Constrained Blind Detection of CDMA Signals in Multipath Channels," *IEEE Sig. Proc. Letters*, vol. 9, No. 12, December 2002.
- [21] R. C. de Lamare and R. Sampaio Neto, "Blind Adaptive Code-Constrained Constant Modulus Algorithms for CDMA Interference Suppression in Multipath Channels", *IEEE Communications Letters*, vol 9. no. 4, April, 2005.
- [22] L. Landau, R. C. de Lamare and M. Haardt, "Robust adaptive beamforming algorithms using the constrained constant modulus criterion," *IET Signal Processing*, vol.8, no.5, pp.447-457, July 2014.
- [23] R. C. de Lamare, "Adaptive Reduced-Rank LCMV Beamforming Algorithms Based on Joint Iterative Optimisation of Filters", *Electronics Letters*, vol. 44, no. 9, 2008.
- [24] R. C. de Lamare and R. Sampaio-Neto, "Adaptive Reduced-Rank Processing Based on Joint and Iterative Interpolation, Decimation and Filtering", *IEEE Transactions on Signal Processing*, vol. 57, no. 7, July 2009, pp. 2503 - 2514.
- [25] R. C. de Lamare and Raimundo Sampaio-Neto, "Reduced-rank Interference Suppression for DS-CDMA based on Interpolated FIR Filters", *IEEE Communications Letters*, vol. 9, no. 3, March 2005.
- [26] R. C. de Lamare and R. Sampaio-Neto, "Adaptive Reduced-Rank MMSE Filtering with Interpolated FIR Filters and Adaptive Interpolators", *IEEE Signal Processing Letters*, vol. 12, no. 3, March, 2005.
- [27] R. C. de Lamare and R. Sampaio-Neto, "Adaptive Interference Suppression for DS-CDMA Systems based on Interpolated FIR Filters with Adaptive Interpolators in Multipath Channels", *IEEE Trans. Vehicular Technology*, Vol. 56, no. 6, September 2007.
- [28] R. C. de Lamare, "Adaptive Reduced-Rank LCMV Beamforming Algorithms Based on Joint Iterative Optimisation of Filters," *Electronics Letters*, 2008.
- [29] R. C. de Lamare and R. Sampaio-Neto, "Reduced-rank adaptive filtering based on joint iterative optimization of adaptive filters", *IEEE Signal Process. Lett.*, vol. 14, no. 12, pp. 980-983, Dec. 2007.
- [30] R. C. de Lamare, M. Haardt, and R. Sampaio-Neto, "Blind Adaptive Constrained Reduced-Rank Parameter Estimation based on Constant Modulus Design for CDMA Interference Suppression", *IEEE Transactions on Signal Processing*, June 2008.
- [31] M. Yukawa, R. C. de Lamare and R. Sampaio-Neto, "Efficient Acoustic Echo Cancellation With Reduced-Rank Adaptive Filtering Based on Selective Decimation and Adaptive Interpolation," *IEEE Transactions on Audio, Speech, and Language Processing*, vol.16, no. 4, pp. 696-710, May 2008.
- [32] R. C. de Lamare and R. Sampaio-Neto, "Reduced-rank space-time adaptive interference suppression with joint iterative least squares algorithms for spread-spectrum systems," *IEEE Trans. Vehi. Technol.*, vol. 59, no. 3, pp. 1217-1228, Mar. 2010.
- [33] R. C. de Lamare and R. Sampaio-Neto, "Adaptive reduced-rank equalization algorithms based on alternating optimization design techniques for MIMO systems," *IEEE Trans. Vehi. Technol.*, vol. 60, no. 6, pp. 2482-2494, Jul. 2011.
- [34] R. C. de Lamare, L. Wang, and R. Fa, "Adaptive reduced-rank LCMV beamforming algorithms based on joint iterative optimization of filters: Design and analysis," *Signal Processing*, vol. 90, no. 2, pp. 640-652, Feb. 2010.
- [35] R. Fa, R. C. de Lamare, and L. Wang, "Reduced-Rank STAP Schemes for Airborne Radar Based on Switched Joint Interpolation, Decimation and Filtering Algorithm," *IEEE Transactions on Signal Processing*, vol.58, no.8, Aug. 2010, pp.4182-4194.
- [36] L. Wang and R. C. de Lamare, "Low-Complexity Adaptive Step Size Constrained Constant Modulus SG Algorithms for Blind Adaptive Beamforming", *Signal Processing*, vol. 89, no. 12, December 2009, pp. 2503-2513.
- [37] L. Wang and R. C. de Lamare, "Adaptive Constrained Constant Modulus Algorithm Based on Auxiliary Vector Filtering for Beamforming," *IEEE Transactions on Signal Processing*, vol. 58, no. 10, pp. 5408-5413, Oct. 2010.
- [38] L. Wang, R. C. de Lamare, M. Yukawa, "Adaptive Reduced-Rank Constrained Constant Modulus Algorithms Based on Joint Iterative Optimization of Filters for Beamforming," *IEEE Transactions on Signal Processing*, vol.58, no.6, June 2010, pp.2983-2997.
- [39] L. Wang, R. C. de Lamare and M. Yukawa, "Adaptive reduced-rank constrained constant modulus algorithms based on joint iterative optimization of filters for beamforming", *IEEE Transactions on Signal Processing*, vol.58, no. 6, pp. 2983-2997, June 2010.

- [40] L. Wang and R. C. de Lamare, "Adaptive constrained constant modulus algorithm based on auxiliary vector filtering for beamforming", *IEEE Transactions on Signal Processing*, vol. 58, no. 10, pp. 5408-5413, October 2010.
- [41] R. Fa and R. C. de Lamare, "Reduced-Rank STAP Algorithms using Joint Iterative Optimization of Filters," *IEEE Transactions on Aerospace and Electronic Systems*, vol.47, no.3, pp.1668-1684, July 2011.
- [42] Z. Yang, R. C. de Lamare and X. Li, "L1-Regularized STAP Algorithms With a Generalized Sidelobe Canceler Architecture for Airborne Radar," *IEEE Transactions on Signal Processing*, vol.60, no.2, pp.674-686, Feb. 2012.
- [43] Z. Yang, R. C. de Lamare and X. Li, "Sparsity-aware spacetime adaptive processing algorithms with L1-norm regularization for airborne radar", *IET signal processing*, vol. 6, no. 5, pp. 413-423, 2012.
- [44] Neto, F.G.A.; Nascimento, V.H.; Zakharov, Y.V.; de Lamare, R.C., "Adaptive re-weighting homotopy for sparse beamforming," in *Signal Processing Conference (EUSIPCO)*, 2014 Proceedings of the 22nd European , vol., no., pp.1287-1291, 1-5 Sept. 2014
- [45] Almeida Neto, F.G.; de Lamare, R.C.; Nascimento, V.H.; Zakharov, Y.V., "Adaptive reweighting homotopy algorithms applied to beamforming," *IEEE Transactions on Aerospace and Electronic Systems*, vol.51, no.3, pp.1902-1915, July 2015.
- [46] L. Wang, R. C. de Lamare and M. Haardt, "Direction finding algorithms based on joint iterative subspace optimization," *IEEE Transactions on Aerospace and Electronic Systems*, vol.50, no.4, pp.2541-2553, October 2014.
- [47] S. D. Somasundaram, N. H. Parsons, P. Li and R. C. de Lamare, "Reduced-dimension robust capon beamforming using Krylov-subspace techniques," *IEEE Transactions on Aerospace and Electronic Systems*, vol.51, no.1, pp.270-289, January 2015.
- [48] S. Xu and R.C de Lamare, , *Distributed conjugate gradient strategies for distributed estimation over sensor networks*, *Sensor Signal Processing for Defense SSPD*, September 2012.
- [49] S. Xu, R. C. de Lamare, H. V. Poor, "Distributed Estimation Over Sensor Networks Based on Distributed Conjugate Gradient Strategies", *IET Signal Processing*, 2016 (to appear).
- [50] S. Xu, R. C. de Lamare and H. V. Poor, *Distributed Compressed Estimation Based on Compressive Sensing*, *IEEE Signal Processing Letters*, vol. 22, no. 9, September 2014.
- [51] S. Xu, R. C. de Lamare and H. V. Poor, "Distributed reduced-rank estimation based on joint iterative optimization in sensor networks," in *Proceedings of the 22nd European Signal Processing Conference (EUSIPCO)*, pp.2360-2364, 1-5, Sept. 2014
- [52] S. Xu, R. C. de Lamare and H. V. Poor, "Adaptive link selection strategies for distributed estimation in diffusion wireless networks," in *Proc. IEEE International Conference on Acoustics, Speech and Signal Processing (ICASSP)*, , vol., no., pp.5402-5405, 26-31 May 2013.
- [53] S. Xu, R. C. de Lamare and H. V. Poor, "Dynamic topology adaptation for distributed estimation in smart grids," in *Computational Advances in Multi-Sensor Adaptive Processing (CAMSAP)*, 2013 IEEE 5th International Workshop on , vol., no., pp.420-423, 15-18 Dec. 2013.
- [54] S. Xu, R. C. de Lamare and H. V. Poor, "Adaptive Link Selection Algorithms for Distributed Estimation", *EURASIP Journal on Advances in Signal Processing*, 2015.
- [55] N. Song, R. C. de Lamare, M. Haardt, and M. Wolf, "Adaptive Widely Linear Reduced-Rank Interference Suppression based on the Multi-Stage Wiener Filter," *IEEE Transactions on Signal Processing*, vol. 60, no. 8, 2012.
- [56] N. Song, W. U. Alokozai, R. C. de Lamare and M. Haardt, "Adaptive Widely Linear Reduced-Rank Beamforming Based on Joint Iterative Optimization," *IEEE Signal Processing Letters*, vol.21, no.3, pp. 265-269, March 2014.
- [57] R.C. de Lamare, R. Sampaio-Neto and M. Haardt, "Blind Adaptive Constrained Constant-Modulus Reduced-Rank Interference Suppression Algorithms Based on Interpolation and Switched Decimation," *IEEE Trans. on Signal Processing*, vol.59, no.2, pp.681-695, Feb. 2011.
- [58] Y. Cai, R. C. de Lamare, "Adaptive Linear Minimum BER Reduced-Rank Interference Suppression Algorithms Based on Joint and Iterative Optimization of Filters," *IEEE Communications Letters*, vol.17, no.4, pp.633-636, April 2013.
- [59] R. C. de Lamare and R. Sampaio-Neto, "Sparsity-Aware Adaptive Algorithms Based on Alternating Optimization and Shrinkage," *IEEE Signal Processing Letters*, vol.21, no.2, pp.225,229, Feb. 2014.
- [60] Fa R., de Lamare R. C., and Wang L., Reduced-rank STAP schemes for airborne radar based on switched joint interpolation, decimation and filtering algorithm, *IEEE Transactions on Signal Processing*, vol.58, no.8, pp.4182-4194, 2010.
- [61] Roman J. R., Rangaswamy M., Davis D. W., Zhang Q., Himed B., Michels J.H., Parametric adaptive matched filter for airborne radar applications, *IEEE Transactions on Aerospace and Electronic Systems*, vol.36, no.2, pp.677-692, 2000.
- [62] Yang Z., de Lamare R. C., and Li X., Sparsity-aware space-time adaptive processing algorithms with L_1 -norm regularization for airborne radar, *IET Signal Processing*, vol.6, no.5, pp.413-423, 2012.
- [63] Yang Z., de Lamare R. C., and Li X., L_1 -regularized STAP algorithms with a generalized sidelobe canceler architecture for airborne radar, *IEEE Transactions on Signal Processing*, vol.60, no.2, pp.674-686, Feb. 2012.
- [64] Guerci J. R., and Baranoski E. J., Knowledge-Aided adaptive radar at DARPA: an overview, *IEEE Signal Processing Magazine*, vol.23, no.1, pp.41-50, 2006.
- [65] Wang P., Wang Z., Li H., and Himed B., Knowledge-Aided Parametric Adaptive Matched Filter With Automatic Combining for Covariance Estimation, *IEEE Transactions on Signal Processing*, vol.62, no.18, pp.4713-4722, 2014.
- [66] Jeong Hwan B., Melvin W.L., and Lanterman A.D., Model-based clutter cancellation based on enhanced knowledge-aided parametric covariance estimation, *IEEE Transactions on Aerospace and Electronic Systems*, vol.51, no.1, pp.154-166, 2015.
- [67] Yang Z., Li X., Wang H., and Fa R., Knowledge-aided STAP with sparse-recovery by exploiting spatio-temporal sparsity, *IET Signal Processing*, vol.10, no.2, pp.150-161, 2016.
- [68] Liu A., Sun H., Teh K. C., Baker C. J., and Gao C., Robust space-time adaptive processing for nonhomogeneous clutter in the presence of model errors, *IEEE Transactions on Aerospace and Electronic Systems*, vol.52, no.1, pp.155-168, 2016.
- [69] Yang Z., and de Lamare R. C., Enhanced knowledge-aided space-time adaptive processing exploiting inaccurate prior knowledge of the array manifold, *Digital Signal Processing*, vol.60, pp.262-276, 2017.
- [70] Sarkar T. K., Wang H., Park S., Adve R., Koh J., Kim K., Zhang Y., Wicks M. C., and Brown R. D., A deterministic least-squares approach to space-time adaptive processing (STAP), *IEEE Transactions on Antennas and Propagations*, vol.49, no.1, pp.91-103, 2001.
- [71] Aboutanios E., and Mulgrew B., Hybrid detection approach for STAP in heterogeneous clutter, *IEEE Transactions on Aerospace and Electronic Systems*, vol.46, no.3, pp.1021-1033, 2010.
- [72] Maria S. , and Fuchs J. J., Application of the global matched filter to STAP data an efficient algorithmic approach, in *Proceedings of IEEE International Conference on Acoustic Speech and Signal Processing*, 2006, pp. 14-19.
- [73] Selesnick I. W., Pillai S. U., Li K. Y., and Himed B., Angle-Doppler processing using sparse regularization, in *Proceedings of IEEE International Conference on Acoustic Speech and Signal Processing*, 2010, pp.2750-2753.
- [74] Li J., Zhu X., Stoica P., and Rangaswamy M., High resolution angle-Doppler imaging for MTI radar, *IEEE Transactions on Aerospace and Electronic Systems*, vol.46, no.3, pp.1544-1556, Jul. 2010.
- [75] Sun H., Lu Y., and Lesturgie M., Experimental investigation of iterative adaptive approach for ground moving target indication, *IEEE CIE International Conference on Radar*, 2011 pp.715-718.
- [76] Sun K., Meng H., Wang Y., and Wang X., Direct data domain STAP using sparse representation of clutter spectrum, *Signal Processing*, vol. 91, no.9, pp.2222-2236, 2011.
- [77] Bai L., Roy S., and Rangaswamy M., Compressive radar clutter subspace estimation using dictionary learning, in *Proceedings of IEEE Radar Conference*, 2013, pp.1-6.
- [78] Yang Z., Qin Y., de Lamare R.C., Wang H., and Li X., Sparsity-based direct data domain space-time adaptive processing with intrinsic clutter motion, *Circuits Systems and Signal Processing*, vol.36, pp.219-246, 2017.
- [79] Sen S., OFDM radar space-time adaptive processing by exploiting spatio-temporal sparsity, *IEEE Transactions on Signal Processing*, vol.61, no.1, pp.118-130, 2013.
- [80] Sun K., Zhang H., Li G., Meng H., and Wang X., A novel STAP algorithm using sparse recovery technique, in *Proceedings of IEEE International Geoscience and Remote Sensing Symposium*, 2009, pp.336-339.
- [81] Yang Z., Li X., Wang H., and W. Jiang, On clutter sparsity analysis in space-time adaptive processing airborne radar, *IEEE Geoscience and Remote Sensing Letters*, vol.10, no.5, pp.1214-1218, 2013.

- [82] Yang Z., Li X., Wang H., and Jiang W., Adaptive clutter suppression based on iterative adaptive approach for airborne radar, *Signal Processing*, vol.93, no.12, pp.3567-3577, 2013.
- [83] Yang Z., Li X., Wang H., and Nie L., Sparsity-based space-time adaptive processing using complex-valued homotopy technique for airborne radar, *IET Signal Processing*, vol.8, no.5, pp.552-564, 2014.
- [84] Sen S., Low-rank matrix decomposition and spatio-temporal sparse recovery for STAP radar, *IEEE Journal of Selected Topics in Signal Processing*, vol.9, no.8, pp.1510-1523, 2015.
- [85] Wu Q., Zhang Y. D., Amin M. G., and Himed B., Space-time adaptive processing and motion parameter estimation in multistatic passive radar using sparse Bayesian learning, *IEEE Transactions on Geoscience and Remote Sensing*, vol.54, no.2, pp.944-957, 2016.
- [86] Wang Z., Wang Y., Duan K., and Xie W., Subspace-augmented clutter suppression technique for STAP radar, *IEEE Geoscience and Remote Sensing Letters*, vol.13, no.3, pp.462-466, 2016.
- [87] Ma Z., Liu Y., Meng H., and Wang X., Sparse recovery-based space-time adaptive processing with array error self-calibration, *Electronics Letters*, vol.50, no.13, pp.152-154, 2014.
- [88] Parker J. T., and Potter L. C., A Bayesian perspective on sparse regularization for STAP post-processing, in *Proceeding of IEEE Radar Conference*, May 2010, pp.1471-1475.
- [89] Kim H. H., Haimovich A. M., and Govoni M. A., Sparse arrays, MIMO, and compressive sensing for GMTI radar, in *Proceeding of Asilomar Conference on Signals, Systems and Computing*, 2014, pp.849-853.
- [90] Kim H. H., Govoni M. A., Haimovich A. M., Cost analysis of compressive sensing for MIMO STAP random arrays, in *Proc. IEEE Radar Conference*, 2015, pp.980-985.
- [91] Yang J., and Zhang Y., Alternating direction algorithms for l_1 -problems in compressive sensing, *SIAM Journal on Scientific Computing*, vol.33, no.1, pp.250-278, 2011.
- [92] Bilen Ç., Puy G., Gribonval R., and Daudet L., Convex optimization approaches for build sensor calibration using sparsity, *IEEE Transactions on Signal Processing*, vol.62, no.18, pp.4847-4856, 2014.
- [93] Bergin J. S., Teixeira C. M., Techau P. M., and Guerci J. R., STAP with knowledge-aided data pre-whitening, in *Proceeding of IEEE Radar Conference*, 2004, pp.289-294.
- [94] [Online]. Available: <http://www.stanford.edu/boyd/cvx>